Mechanics of Materials 53 (2012) 15–28

Contents lists available at SciVerse ScienceDirect

Mechanics of Materials

journal homepage: www.elsevier.com/locate/mechmat

Three different approaches for damage domain characterization in disordered materials: Fractal energy density, *b*-value statistics, renormalization group theory

Alberto Carpinteri, Mauro Corrado *, Giuseppe Lacidogna

Department of Structural Engineering and Geotechnics, Politecnico di Torino, Corso Duca degli Abruzzi 24, 10129 Torino, Italy

ARTICLE INFO

Article history:
Received 1 March 2011
Received in revised form 2 May 2012
Available online 17 May 2012

Keywords:
Compressive failure
Fracture pattern
Fractals
Acoustic emission
b-Value analysis
Renormalization group theory

ABSTRACT

Material characterization is usually based on the stress–strain constitutive laws directly derived from the load–displacement relations of uniaxial compression tests. This approach, which implies a uniform distribution of deformation along the specimen axis and an energy dissipation within a volume, does not permit to correctly describe the mechanical behavior and the damage evolution by varying the structural size and slenderness.

In this paper, three different approaches are used to evaluate the physical dimension of the damage domain in disordered materials subjected to uniaxial compression. The energetic and the statistical methods are based on the acoustic emission monitoring technique, whereas the renormalization group procedure is based on the assumption of anomalous physical dimensions for the material properties. The three approaches agree very well in the determination of the damage domain fractal dimension.

1. Introduction

Damage and fracture characterizing the compressive failure of heterogeneous materials such as rocks and concrete are complex processes involving wide ranges of time and length scales, from the micro- to the structural-scale. They are governed by the nucleation, growth and coalescence of microcracks and defects, eventually leading to the final collapse, and to the loss of the classical mechanical parameters, such as nominal strength, dissipated energy density and deformation at failure, as material properties. For instance, it is well-established from experiments that a strong localization of deformations occurs in the post-peak regime, and the energy dissipation is a surface-dominated phenomenon, in close analogy with the behavior in tension (see the experimental results by Hudson et al. (1972) for rocks, and by Kotsovos (1983) and van Mier (1984) for concrete). According to these evidences, the *Overlapping Crack Model* has been proposed by Carpinteri et al. (2007a, 2009a) for modeling the crushing process in concrete-like materials. Such a model, analogously to the *Cohesive Crack Model* routinely adopted for quasi-brittle materials in tension, assumes a stress–displacement (fictitious interpenetration) law as a material property for the post-peak behavior, to which corresponds an energy dissipation over a surface. This simple model has permitted to explain the well-known size and slenderness effects on the structural ductility, characterizing the mechanical behavior of concrete-like materials subjected to uniaxial and eccentric compression tests (Carpinteri et al., 2009a, 2011a).

On the other hand, the assumption of an energy dissipation over a surface is just an effective idealization of a more complex mechanism characterized by diffused macrocracks after the coalescence of initial microcracks. An accurate description of such a reality cannot be done on the basis of the classical continuum mechanics, and modeling fracture and failure of a material with heterogeneous microstructures, as, for example, rocks and concrete, thus

* Corresponding author. Tel.: +39 011 5644873; fax: +39 011 5644899.
E-mail address: mauro.corrado@polito.it (M. Corrado).

0167-6636/$ - see front matter © 2012 Elsevier Ltd. All rights reserved.
http://dx.doi.org/10.1016/j.mechmat.2012.05.004

requires use of fractals or multifractals (Carpinteri, 1994a), and renormalization group theory (Carpinteri, 1994b). The fractal approach has proven to be very effective; as the 'geometry of nature' (Mandelbrot, 1982), fractals provide a powerful approach not only to quantitatively describe irregular fracture surfaces (Mandelbrot et al., 1984; Carpinteri et al., 1999), but also a means to establish a bridge between micromechanical damage and macromechanical behavior.

Among others, we could cite the work by Chelidze and Gueguen (1990) that explains the physical properties of fractal systems and the way they affect the measured values of surface fracture energy. We also mention the papers by Krajcinovic and Rinaldi (2005) and Rinaldi et al. (2006), where a connection between damaged random heterogeneous micromaterial and the system macroparameter is sought and the fractal dimension is used to propose constitutive relations and scaling laws. Panin et al. (2002) investigated the formation of fractal patterns at the meso-level in a multi-scale approach to fracture; Carpinteri (1994a,b) and Carpinteri et al. (2002) addressed the fundamental issue of the size-scale effects on material strength, toughness and critical strain, which are seen as the result of damage localization of the failure mechanisms over fractal patterns.

Investigations with the acoustic emission (AE) technique of micro-fracture processes have also revealed power-law distributions and critical phenomena (King, 1983; Hirata, 1989; Main, 1991, 1992, 2000; Sammonds et al., 1994; Garcimartin et al., 1997; Sethna et al., 2001; Colombo et al., 2003; Rundle et al., 2003; Carpinteri et al., 2006b) characterized by intermittency of AE event avalanches, fractal distributions of AE event locations, and complex space–time coupling (Lu et al., 2005). Localization of cracks distribution within the specimen volume by means of the AE technique has also permitted to physically confirm that the energy is dissipated over preferential bands and surfaces during the damage evolution (Carpinteri et al., 2008a,b, 2010; Weiss and Marsan, 2003).

In the present paper, three different approaches are proposed to obtain indirect estimation of the physical dimension of the damage domain up to the peak load and in the post-peak regime of quasi-brittle materials, such as concrete and rocks, subjected to compression. First, an energy density approach is presented, based on the size-effects on the energy release determined by the AE technique. This calculation is performed by considering specimens with different size-scale. Then, a complementary method is proposed, based on the *b*-value analysis of AE events. Since the *b*-value is size-independent, its evaluation evidences the similarity between the damage process in a structure and the seismic activity in a region of the earth crust (Scholz, 1968). Finally, in the third method, the physical dimension of the damage domain is computed in order to obtain scale-independent constitutive laws for the softening regime. In this case, the analysis is carried out from the experimental data of specimens with different diameters and slenderness. The results obtained from these three different approaches will be compared and the good agreement between them will be emphasized.

The main novelty of this study is that – despite the three proposed approaches have already been separately described by the Authors in previous papers dealing with disordered materials subjected to uniaxial compression – a synthesis work highlighting the common or different consequences in the evaluation of the physical dimension of the damage domain was never written before.

2. Energy density criterion for the evaluation of the damage domain fractal dimension

2.1. Energy release detection by acoustic emission

Monitoring a structure by means of the AE technique, it proves possible to detect the occurrence and evolution of stress-induced cracks. Cracking, in fact, is accompanied by the emission of elastic waves which propagate within the bulk of the material. These waves can be received and recorded by transducers applied to the surface of structural elements. This technique, originally used to detect cracks and plastic deformations in metals, has been extended to studies in the field of rocks and concrete, and it can be used for the diagnosis of structural damage phenomena (Ohtsu, 1996). Recently, AE data have been interpreted by means of statistical and fractal analysis, considering the multiscale aspect of cracking phenomena (Carpinteri et al., 2007b). This approach has shown that the energy release, detected by AE, occurs in a fractal (lacunar) domain with a dimension lower than 3. Consequently, a multiscale criterion to predict the damage evolution has been formulated.

Recent developments in fragmentation theories (Carpinteri and Pugno, 2002a,b), have shown that the energy W during microcrack propagation is released over a fractal domain comprised between a surface and the specimen volume V. As a result, the following size-scaling law has been assumed for the energy release W during fragmentation:

$$W \propto V^{D/3}, \tag{1}$$

where D is the so-called fractal exponent, comprised between 2 and 3. As a consequence, the energy density scales as

$$\Psi = \frac{W}{V} \propto V^{(D-3)/3}. \tag{2}$$

This implies that not the true energy density but a fractal energy density (having non-integer physical dimensions)

$$\Gamma = \frac{W}{V^{D/3}} \tag{3}$$

can be considered as the size-independent parameter.

On the other hand, during microcrack propagation, AE can be clearly detected. The energy release W is proportional to the number N of AE events. Accordingly to the energy release from a fractal domain, as described by Eq. (3), the number of AE events, N, not over a volume but over a fractal domain, can be considered as the size-independent parameter:

$$\Gamma_{\mathrm{AE}} = \frac{N}{V^{D/3}}, \tag{4}$$

where Γ_{AE} is the value of AE events fractal density. The fractal criterion in Eq. (4), permits to extend Eq. (1) as follows:

$$W \propto N \propto V^{D/3}. \tag{5}$$

2.2. Experimental assessment

The experimental validation of the theoretical conjecture herein considered is performed on the basis of the results of uniaxial compression tests carried out on cylindrical concrete and rock specimens. The concrete samples were drilled from two pilasters sustaining a viaduct along an Italian highway built in the 1950s (Carpinteri et al., 2007b). Three different specimen diameters d in a scale range 1.0:2.1:3.4 (d = 27.7, 59.0 and 94.0 mm) and three different slendernesses, $\lambda = h/d$, equal to 0.5, 1.0 and 2.0 were considered. The nine geometries are shown in Fig. 1a. The tests were performed under displacement control, assuming a displacement rate equal to 10^{-4} mm/s, in order to obtain slow crack growth and to detect all possible AE signals. The load was applied by means of rigid steel platens without friction-reducing systems.

The second experimental campaign herein considered concerns the compression tests carried out on rock samples taken from one pillar of the Cathedral of Syracuse, in Sicily. They were drilled from removed elements replaced by other blocks during restoration works. The pillars of the Cathedral have the peculiar interest that they had been obtained by cutting out the stonework walls of the internal cell of the 5th Century B.C. Greek temple of Athena. In the 6th Century, it was transformed into a Catholic Church, and then frequently modified until the present configuration. More in detail, the ancient stone used in the construction of the temple was a calcareous stone located in the area of Plemmirio, just south of Syracuse. Specimens with diameters d in a scale range 1:2:4 (d = 30, 60 and 120 mm), and slenderness λ = 1, were tested (Fig. 2a). The specimens were subjected to laboratory compressive tests at constant displacement rate of 4×10^{-4}mm/s and monitored by the AE technique (Carpinteri et al., 2011b). The load was applied by means of rigid steel platens without friction-reducing systems. The results evidenced an average compressive strength equal to 8.20 MPa, with variations due to statistics rather than to clear size-effects.

For all the tested specimens, the number of AE was evaluated in correspondence to the peak stress σ_c, and, in the following, referred to as N_{max}. This analysis is performed

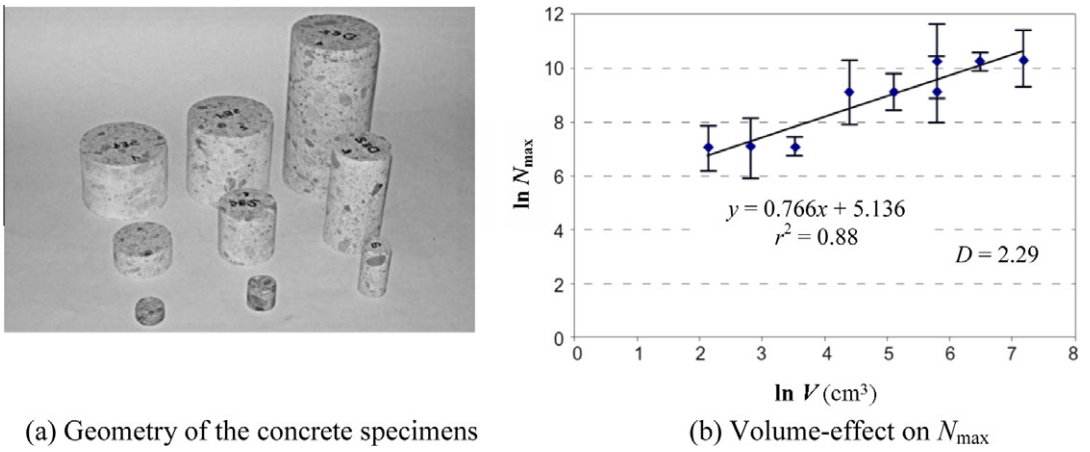

Fig. 1. Concrete specimens tested by Carpinteri et al. (2007b): geometry (a) and volume-effect on N_{max} (b).

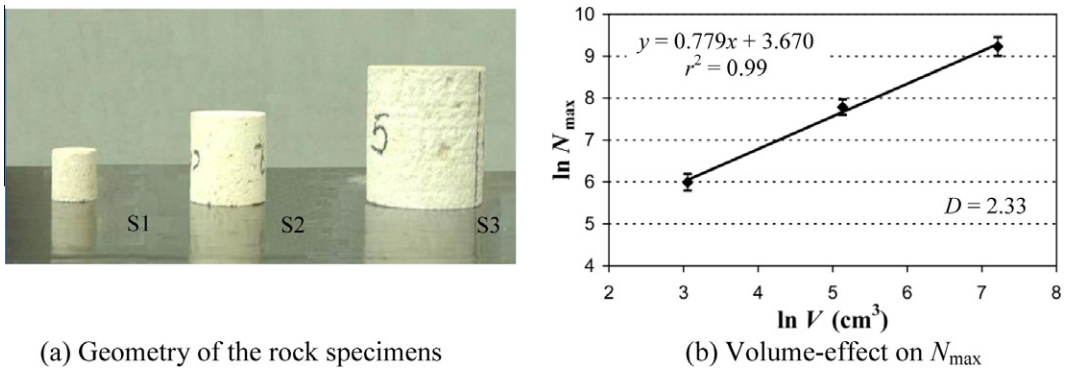

Fig. 2. Rock specimens tested by Carpinteri et al. (2011b): geometry (a) and volume-effect on N_{max} (b).

by a measuring system counting the events that exceed a certain voltage threshold measured in volts. On average, compression tests show an increase in AE cumulative events number by increasing the specimen volume, as shown in Figs. 1b and 2b. Subjecting the average experimental data to a regression analysis, the parameter D in Eq. (4) can be quantified. The parameter $D/3$ represents the slope, in the bi-logarithmic diagram, of the curve that relates N_{max} to the specimen volume. From the best-fitting, values of $D/3$ equal to 0.766 and 0.779 were obtained for concrete and rocks specimens, respectively (see Figs. 1b and 2b). The corresponding fractal exponents, D, result to be 2.29 and 2.33, respectively. The goodness of fit for the best-fitting curve in Fig. 1b is $r^2 = 0.88$, while in Fig. 2b is $r^2 = 0.99$.

The experimental results reported in Figs. 1b and 2b confirm that the energy release is proportional to the cumulative acoustic emission events and, according to fragmentation theories, it takes place in a fractal domain intermediate between a surface and a volume, instead of small defects homogeneously distributed within the volume. From these assumptions, considering that N_{max} is the total number of AE events evaluated at the peak stress σ_c under compression, a size-independent fractal density Γ_{AE} can be defined, as the intercept of the best-fitting curve in Figs. 1b and 2b. Its physical dimension is proportional to L^{-D}. Once its value and the slope D of the scaling law are known, the energy release at the peak stress from specimens with different sizes can be predicted.

2.3. Materials properties and test conditions

Even though the two considered materials, concrete an rocks, are characterized by very different values for the mechanical parameters, such as strength and dissipated energy, the dimensions of the damage domain are almost the same. At this regard, it is worth noting that the considered limestone rock is characterized by a coarse microstructure, similar to that of concrete. Moreover, these specimens were neither pre-cracked nor characterized by preferential cracking surfaces, and therefore the damage fractal dimension is not influenced by the geometrical character and orientation of pre-existing joints.

As for the type of compression tests, using stiff platens, due to end constraints, friction affects the stress field inducing radial compressive stresses close to the specimen ends: the higher is the h/d ratio, the faster these effects vanish far from the ends (see Carpinteri et al., 2007b). On the other hand, a different situation would emerge for softer loading platens, equipped, for example, with a thin layer of Teflon in contact between the platen and the specimen. In this case, the platens would cause a lateral deformation, giving rise to outward-directed shear forces at the interface. When the frictional forces are directed outward, a splitting type of failure is often evidenced entailing the transition from crushing to splitting for uniaxially compressed specimens.

Nevertheless, these phenomena, as already demonstrated in Carpinteri et al. (2007b), have a small influence on the AE events obtained during the compression tests. As a matter of fact, the number of AE events N_{max} has been evaluated in correspondence to the peak stress, and, as a rule, the platens confinement effects become more noticeable only in the post-peak stages.

All the considered compression tests have been carried out without friction-reducers, except for the tests by Ferrara and Gobbi (1995) reported in Section 4.2. "Fractal Overlapping Crack Model". In this case, Teflon layers have been introduced between specimen and loading platens.

3. Damage evolution on the basis of the statistical distribution of AE events

3.1. Acoustic emission statistics

Extensive study on fracture of brittle materials by means of AE technique have shown that damage and fracture growth can be characterized through the b-value of the Gutenberg–Richter (GR) law, which changes systematically during the different stages of the failure process. This parameter can be linked to the value of the exponent of the power-law distribution of the crack size in a damaged medium. A statistical interpretation to the variation of the b-value during the evolution of damage detected by AE has been proposed (Carpinteri et al., 2008b), which is based on a treatment originally proposed by Carpinteri and co-workers (Carpinteri, 1994a; Carpinteri et al., 2008a). The proposed model captures the transition from the condition of diffused criticality to that of imminent failure localization.

By analogy with seismic phenomena, in the AE technique the magnitude may be defined as follows:

$$m = Log_{10} A_{max} + f(r) \tag{6}$$

where A_{max} is the amplitude of the signal expressed in volts, and $f(r)$ is a correction taking into account that the amplitude is a decreasing function of the distance r between the source and the sensor.

In seismology the empirical Gutenberg–Richter's law (Richter, 1958):

$$Log_{10} N(\geqslant m) = a - bm, \quad \text{or} \quad N(\geqslant m) = 10^{a-bm} \tag{7}$$

expresses the relationship between magnitude and total number of earthquakes in any given region and time period, and it is one of the most widely used statistical relations to describe the scaling properties of seismicity. In Eq. (7), N is the cumulative number of earthquakes with magnitude $\geqslant m$ in a given area and within a specific time range, whilst a and b are positive constants varying from a region to another and from a time interval to another. Eq. (7) has been used successfully in the AE field to study the scaling laws of AE wave amplitude distribution. This approach evidences the similarity between structural damage phenomena and seismic activities in a given region of the Earth's crust, extending the applicability of the Gutenberg–Richter's law to Structural Engineering. According to Eq. (7), the b-value changes systematically at different times in the course of the damage process and therefore can be used to estimate damage evolution modalities.

Eq. (7) can be rewritten in order to draw a connection between the magnitude m and the size L of the defect

associated with a AE event. By analogy with seismic phenomena, the AE crack size-scaling entails the validity of the relationship:

$$N(\geqslant L) = cL^{-2b}, \tag{8}$$

where N is the cumulative number of AE events generated by source defects with a characteristic linear dimension $\geqslant L$, c is a constant of proportionality, and $2b = D$ is the fractal dimension of the damage domain.

Aki (1981) was the first to show that the seismic b-value is related to the fractal dimension D, and that usually $2b = D$. This assumption – and its implication with the damage energy release rate and time dependent mechanisms, both at the laboratory and at the Earth's crust scale – has been also pointed out by Main (1991, 1992, 2000). Moreover, it has been evidenced that this interpretation rests on the assumption of a dislocation model for the seismic source and requires that $2.0 \leqslant D \leqslant 3.0$, i.e., the cracks are distributed in a fractal domain comprised between a surface and the volume of the analyzed region (King, 1983; Hirata, 1989; Rundle et al., 2003; Turcotte, 1997).

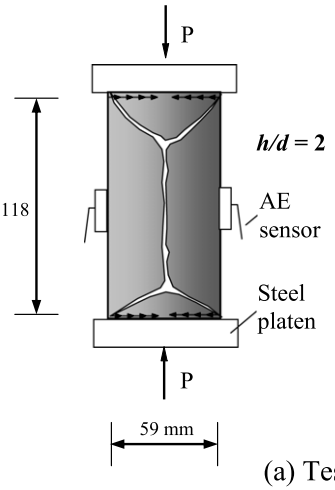

(a) Testing set-up

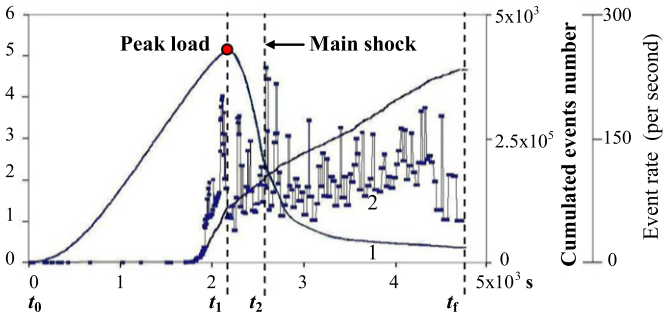

(b) Load 1; Event rate 2; Cumulated events number 3

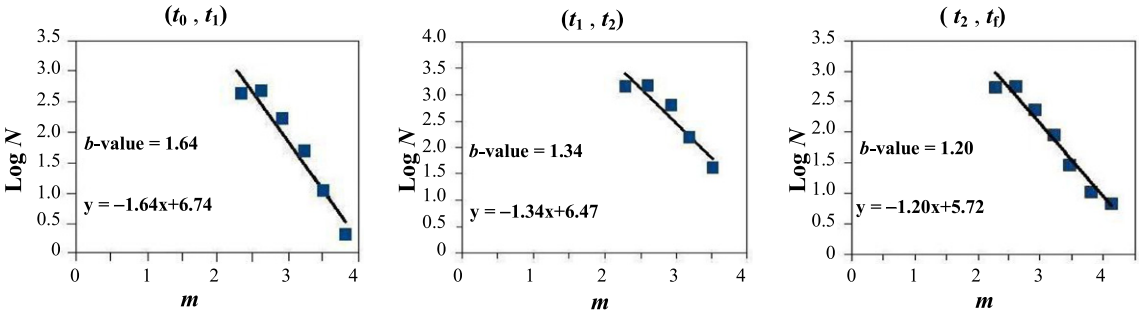

(c) b-values

Fig. 3. Cylindrical concrete specimen in compression by Carpinteri et al. (2007b): testing set-up, with an AE sensor clearly visible on the lateral surface of the specimen (a); load vs. time diagram and AE activity (b) and b-values during the test (c).

The cumulative distribution (8) is substantially identical to the cumulative distribution proposed by Carpinteri (1986, 1994a), which gives the probability of a defect with size $\geqslant L$ being present in a body:

$$P(\geqslant L) \propto L^{-\gamma}. \tag{9}$$

Therefore, the number of defects with size $\geqslant L$ is:

$$N^*(\geqslant L) \sim cL^{-\gamma}, \tag{10}$$

where γ is a statistical exponent measuring the degree of disorder, i.e. the scatter in the defect size distribution, and c is a constant of proportionality. By equating distributions (8) and (10) it is found that: $2b = \gamma$. At the collapse, the size of the maximum defect is proportional to the characteristic size of the structure. As shown by Carpinteri et al. (2008a), the related cumulative defect size distribution (referred to as self-similarity distribution) is

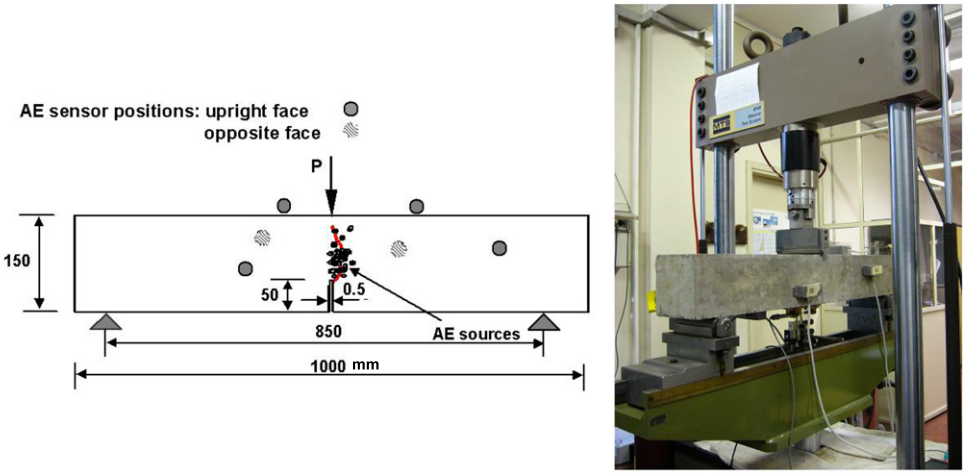

(a) Testing set-up

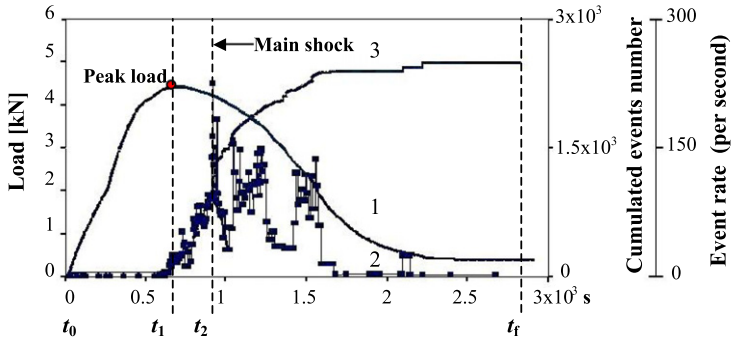

(b) Load 1; Event rate 2; Cumulated events number 3

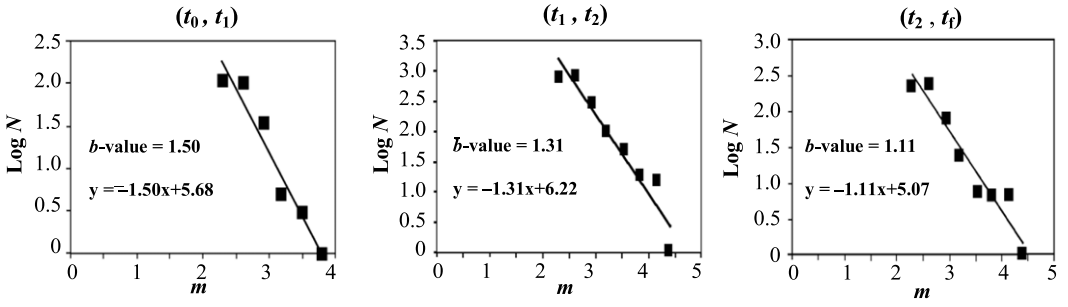

(c) b-values

Fig. 4. Three-point bending test by Carpinteri et al. (2009b,c): specimen geometry, sensor positions and identification of the fracture by the localized AE sources (black points) (a); lad vs. time diagram and AE activity (b) and b-values during the test (c).

characterized by the exponent $\gamma = 2.0$, which corresponds to $b = 1.0$. It was also demonstrated by Carpinteri (1994a) that $\gamma = 2.0$ is a lower bound which corresponds to the minimum value $b = 1.0$, observed experimentally when the load bearing capacity of a structural member has been exhausted.

Therefore, by determining the b-value it is possible to identify the energy release modalities in a structural element during the monitoring process. The extreme cases envisaged by Eq. (7) are $D = 3.0$, which corresponds to the critical conditions $b = 1.5$, when the energy release takes place through small defects homogeneously distributed throughout the volume, and $D = 2.0$, which corresponds to $b = 1.0$, when energy release takes place on a fracture surface. In the former case diffused damage is observed, whereas in the latter two-dimensional cracks are formed leading to the separation of the structural element.

3.2. Statistical distribution of AE events: b-value analysis

The analysis of the b-value during the compression test was carried out for one of the 59 mm diameter concrete specimens with slenderness equal to 2.0 taken from the pilaster of the Italian highway viaduct and presented in Section 2.2. In order to perform this analysis, information about the signal magnitude are required, instead of events counting only. The b-value is the negative gradient of the log-linear AE frequency vs. magnitude diagram and hence it represents the slope of the amplitude distributions (Colombo et al., 2003; Carpinteri et al., 2008a, Rao and Prasanna Lakshmi, 2005). Compressive load versus time, cumulated event number, and event rate for each second of the testing time are depicted in Fig. 3a. The load–time diagram was subdivided into three stages: a first stage (t_0, t_1) extending from initial time to peak load, a second stage (t_1, t_2) going from peak load to mainshock, as identified by the maximum value of the acoustic emission rate, and a third stage (t_2, t_f) going from mainshock to end of the process. The b-values obtained for each stage are shown in Fig. 3b. They range from 1.64 to 1.20. At the beginning of the loading process, the energy release takes place mostly through the formation of microcracks scattered throughout the volume of the material ($b \cong 1.64, D \to 3.0$); at the end of the process, instead, the energy release is seen to concentrate into a two-dimensional crack of a size comparable to that of the specimen, which brings about its separation ($b \cong 1.20, D \to 2.0$).

Similar results were obtained for different geometries and loading conditions. In particular, the single edge notched concrete beam subjected to three-point bending test at the laboratory scale and shown in Fig. 4a, is herein considered. During the loading test, AE generation was monitored by five sensors and the source location procedure was applied to identify the fracture process zone, as shown in Fig. 4a. Nucleation in the fracture process zone might be correlated with the AE clusters zone, and AE clusters are seen to propagate with increasing load (Carpinteri et al., 2009b,c). The load vs. time diagram for the specimen, characterizing the AE activity, is shown in Fig. 4b. Also in this case, the b-values obtained for the three considered stages are in good agreement with the proposed approach: they range from 1.50 to 1.11 (see Fig. 4c). The lower value is obtained in the softening branch of the load-time diagram, and it is very close to 1.0, since the complete separation of the specimen into two parts is approached. Moreover, the fractal dimension of the damage domain, represented by the crack network located by AE technique, has been directly evaluated using the box-counting method. The first stage (t_0, t_1) has not been considered, due to insufficient number of localized points for fractal analysis. The box-counting dimension D reached the value of 2.17 in the intermediate stage (t_1, t_2), and 2.04 in the final stage (t_2, t_f). Such results represent a further confirmation to the effectiveness of Eq. (8) (Carpinteri et al., 2009b).

4. Scale-independent constitutive laws

4.1. Overlapping Crack Model

Damage localization strongly affects the behavior of heterogeneous materials in compression, with particular regard to the post-peak regime (Hudson et al., 1972; van Mier, 1984; Jansen and Shah, 1997). According to several experimental evidences, the Overlapping Crack Model proposed by Carpinteri et al. (2007a) describes the inelastic deformation due to material damage in the softening regime by means of a fictitious interpenetration of the material, while the bulk material undergoes an elastic unloading. As a result, it introduces a couple of constitutive laws in compression, in close analogy with the Cohesive Crack Model: a stress–strain relationship until the compressive strength, σ_c, is achieved (Fig. 5a), and a stress–displacement (*overlapping*) relationship describing the material crushing and expulsion (Fig. 5b). The latter law describes how the stress in the damaged material decreases by increasing the interpenetration displacement, up to a residual value, σ_r, at the critical value, w_{cr}. The area below the stress–overlapping displacement curve of Fig. 5b represents the crushing energy, $\mathcal{G}_C$, which can be assumed as a size-independent material property.

According to the Overlapping Crack Model, the mechanical behavior of a specimen subjected to uniaxial compression (see Fig. 6) can be described by three schematic stages. A first stage where the behavior is mainly characterized by the elastic modulus of the material: a

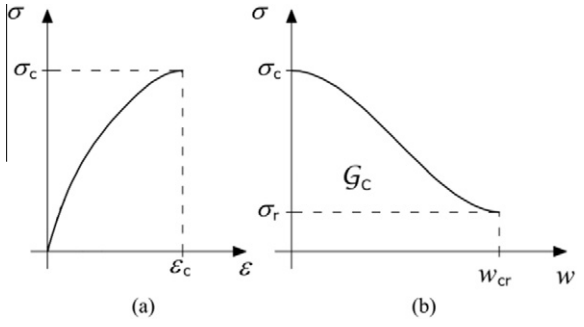

Fig. 5. Overlapping Crack Model: pre-peak stress–strain curve (a) and post-peak stress–overlapping displacement law (b).

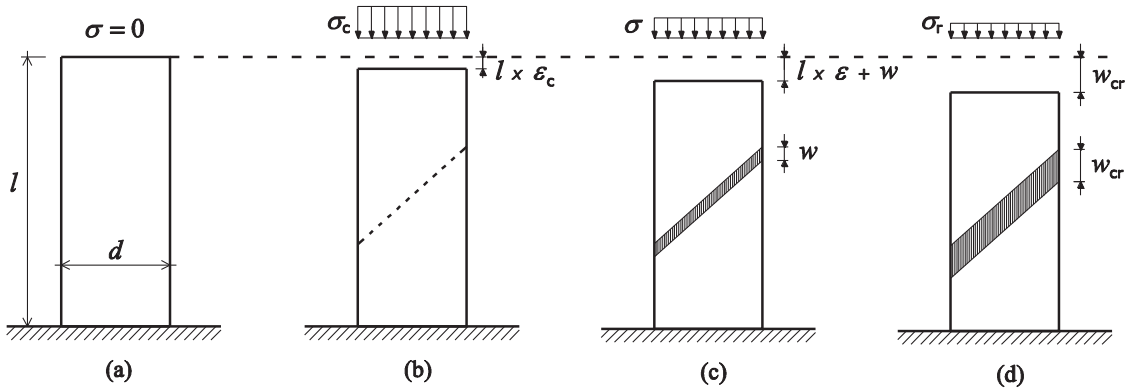

Fig. 6. Subsequent stages in the deformation history of a specimen in compression.

simple linear elastic stress–strain law can be assumed, or even more complicated nonlinear relationships, taking into account energy dissipation within the volume due to initiation and propagation of microcracks (see Fig. 6b). By approaching the compressive strength, such microcracks interact forming macrocracks, and, eventually, localizing on a preferential surface. A second stage where, after reaching the ultimate compressive strength, σ_c, the inelastic deformations are localized in a crushing band. The behavior of this zone is described by the softening law, Fig. 5b, whereas the rest of the specimen still behaves elastically (see Fig. 6c). The displacement of the upper side can be computed as the sum of the elastic deformation and the interpenetration displacement w:

$$\delta = \varepsilon l + w; \quad \text{for } w \leqslant w_{cr}, \tag{11}$$

where l is the specimen length. Both ε and w are functions of the stress level, according to the corresponding constitutive laws shown in Fig. 5. While the crushing zone overlaps, the elastic zone expands at progressively decreasing stresses. When $\delta \geqslant w_{cr}$, in the third stage, the material in the crushing zone is completely damaged and is able to transfer only a constant residual stress, σ_r (see Fig. 6d). As a result, very different global responses in the σ–δ diagram can be obtained by varying the mechanical and geometrical parameters of the sample. In particular, the softening process is stable under displacement control, only when the slope $d\sigma/d\delta$ in the softening regime is negative, Fig. 7a. A sudden drop in the load bearing capacity under displacement control takes place when the slope is infinite, Fig. 7b. Finally, the snap-back instability is avoided, Fig. 7c, if the loading process is controlled by means of the localized interpenetration or the circumferential strain, the slope $d\sigma/d\delta$ of the softening branch being positive. When linear relationships are assumed for the elastic and softening constitutive laws in Fig. 5, by means of simple analytical developments (see Carpinteri and Corrado, 2009 for more details) a snap-back instability is obtained when:

$$\frac{s_E^c}{\varepsilon_c \lambda} \leqslant \frac{1}{2}, \tag{12}$$

where $\lambda = l/d$ is the specimen slenderness, ε_c is the elastic strain recovered during the softening unloading, and $s_E^c = \mathcal{G}_C/\sigma_c d$ is the *energy brittleness number in compression*, proposed by Carpinteri et al. (2009a, 2011a).

An extended validation of the Overlapping Crack Model for concrete-like materials has been presented by Carpinteri et al. (2011a), for specimens with different slendernesses and/or sizes. In general, the post-peak σ–w relationships can be computed from the σ–δ diagrams by subtracting the elastic elongation, caused by the reduction of the applied stress in the post-peak regime, δ_{el}, and the pre-peak plastic deformation, δ_{pl}, as shown in Fig. 8. The experimental stress vs. overlapping displacement curves obtained for the rock specimens extracted from the pillar

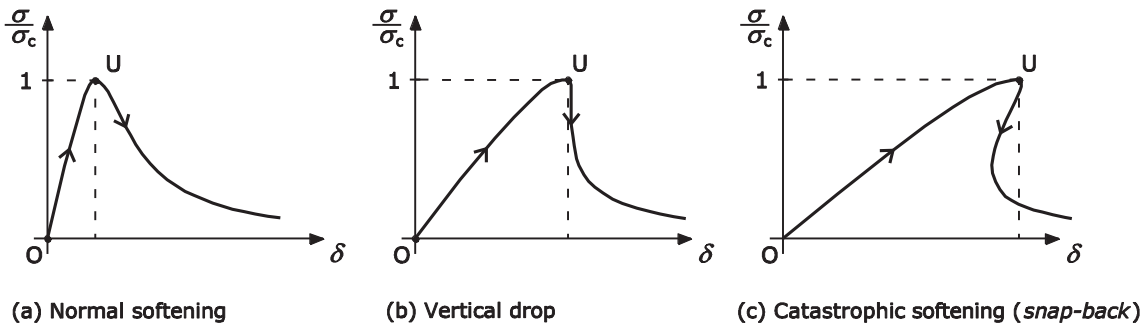

Fig. 7. Stress–displacement response of a specimen in compression.

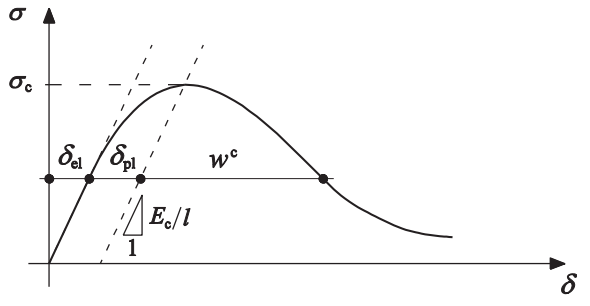

Fig. 8. Estimation of the localized interpenetration, w, from the total shortening of the specimen, δ.

of the Syracuse Cathedral and considered in this study (see Section 2.1), are shown in Fig. 9b. A substantial collapse of the curves onto a narrow band is obtained in comparison to the stress–strain diagrams in Fig. 9a, extending the applicability of the σ–w relationship also to rock materials.

4.2. Fractal Overlapping Crack Model

The assumption of the Overlapping Crack Model that the energy dissipation takes place over a surface is close to the reality, although representing a simplification of a more complex mechanism. A dissipation within a multi-scale or fractal domain is more consistent with the real crushing failure. Accordingly, constant values for the mechanical properties can be obtained only if the classical physical dimensions are abandoned to advantage of non-integer physical dimensions (Carpinteri and Cornetti, 2002; Carpinteri et al., 2006a).

As regards the compressive strength, a fractal parameter can be obtained if a stochastic lacunar set of fractal dimension $2 - d_\sigma$ is adopted to represent the resisting cross-section (of a fractal measure A^*_{res}) of the specimen at the critical load, characterized by the presence of voids and cracks (Fig. 10a):

$$F = \sigma_c A_0 = \sigma^*_c A^*_{res}, \tag{13}$$

where A_0 is the nominal cross-section area, and σ^*_c is the true scale invariant material parameter. The nominal strength σ_c is subjected to a scale effect described by the following negative power-law (Carpinteri, 1994a):

$$\sigma_c \sim \sigma^*_c d^{-d_\sigma}. \tag{14}$$

The exponent of the power law, d_σ, can vary between 0, which corresponds to the homogeneous regime (large

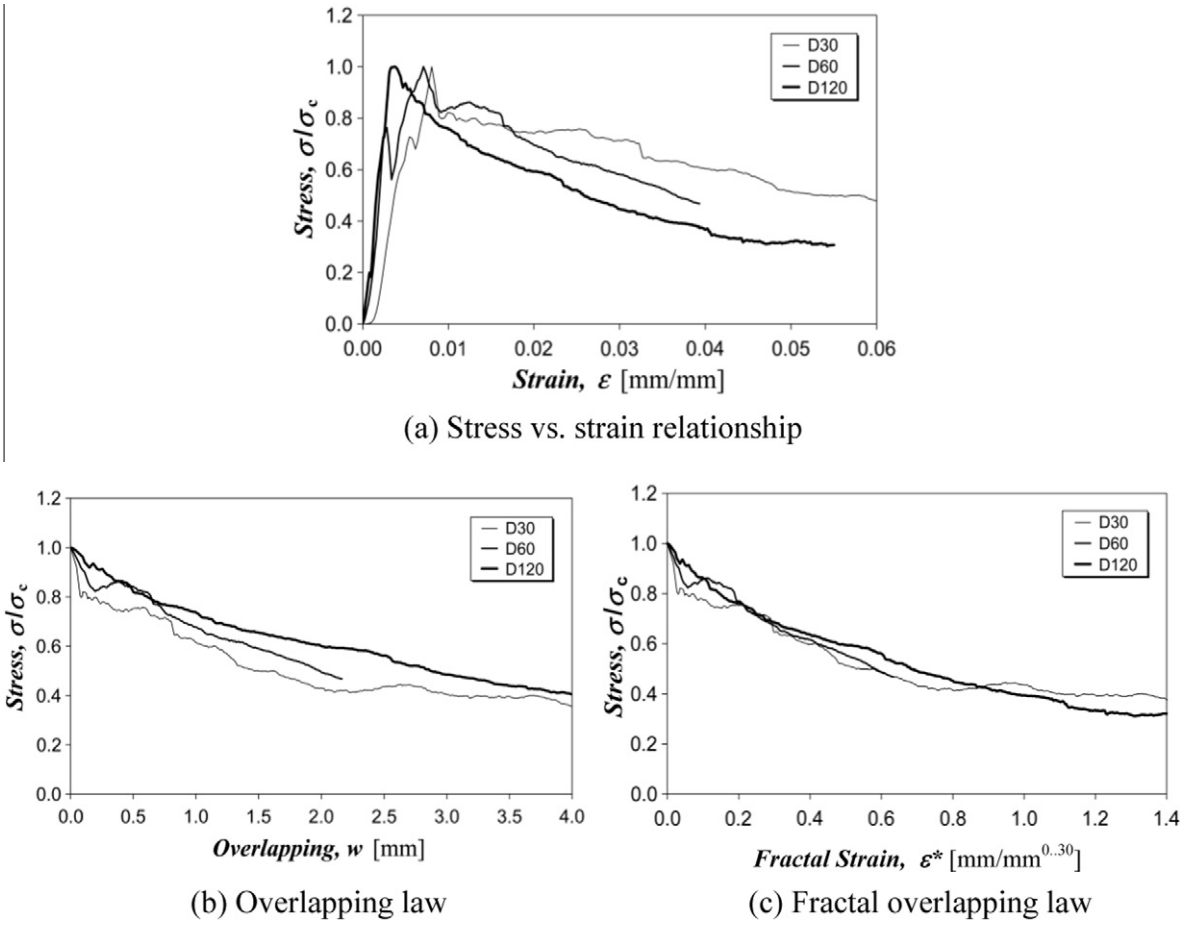

Fig. 9. Compression tests on rock specimens by Carpinteri et al. (2011b): stress vs. strain relationships (a); overlapping law diagrams (b) and fractal overlapping law diagrams (c).

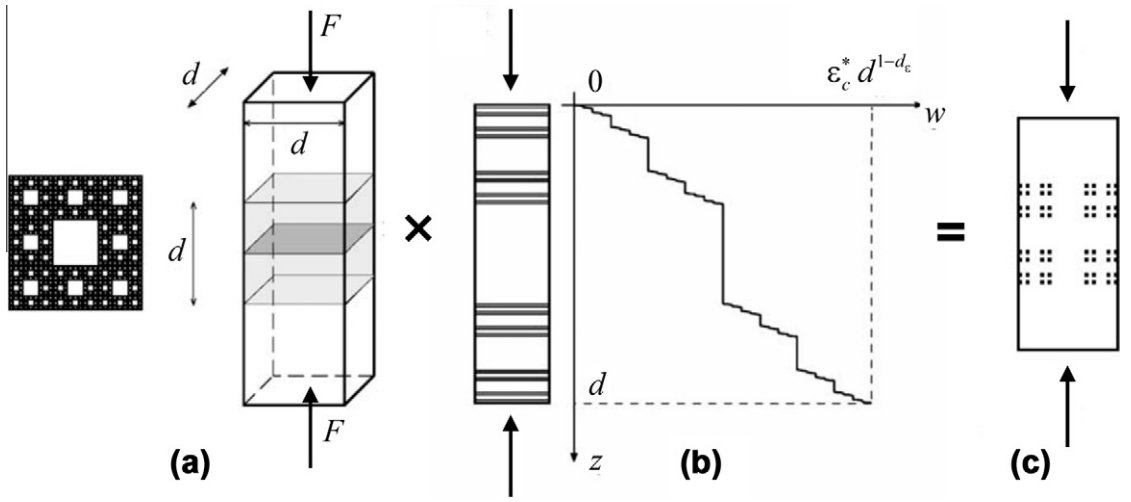

Fig. 10. Fractal localization of stress (a); strain (b) and energy dissipation (c).

scale), and 0.5, which corresponds to the extremely disordered fractal regime (small scale).

A similar argument holds for the crushing energy. In this case, it is assumed that the surface where energy is dissipated is the surface of the aggregates inside the damage band (Fig. 10c), instead of the flat cross-section. Therefore, finite values of the measure of the set where energy is dissipated can be achieved only considering stochastic invasive sets of fractal dimension $2 + d_G$ and fractal measure A^*_{dis}. Therefore, we have:

$$W = \mathcal{G}_C A_0 = \mathcal{G}^*_C A^*_{dis}, \tag{15}$$

where $\mathcal{G}^*_C$ is the true invariant material parameter. The nominal value $\mathcal{G}_C$ is subjected to a scale effect described by the following positive power-law (Carpinteri, 1994a):

$$\mathcal{G}_C \sim \mathcal{G}^*_C d^{+d_\mathcal{G}}. \tag{16}$$

Again, the exponent of the power law, $d_\mathcal{G}$, can vary between 0, corresponding to the homogeneous regime (large scale), and 0.5, corresponding to the extremely disordered fractal regime (small scale).

Finally, fractal sets can be also used to represent the deformation distributions inside the specimen, as experimentally evidenced in metals as well as in rock specimens (Kleiser and Bocek, 1986; Poliakov et al., 1995). In particular, the damage band can be represented by means of a bar subjected to compression (Fig. 10b), where, at the maximum load, contraction strain tends to concentrate into different softening regions, while the rest of the body undergoes elastic unloading. In order to avoid the strain defined in the classical manner becoming meaningless in the singular points, as it diverges, a fractal strain ε^*_c, with anomalous dimension $[L]^{d_\varepsilon}$, is introduced, that, multiplied by the Hausdorff measure of the Cantor set, gives the total shortening of the band at rupture:

$$w_{cr} = \varepsilon_c d = \varepsilon^*_c d^{(1-d_\varepsilon)}. \tag{17}$$

The critical fractal strain is the true material constant, since it is the only scale-invariant parameter governing the kinematics of the fractal band, whereas the nominal value w_{cr} is subjected to a scale effect described by a positive power-law with exponent $1 - d_\varepsilon$ (Carpinteri et al., 2002). The fractional exponent d_ε is intimately related to the degree of disorder in the mesoscopic damage process, and it can vary between 1, corresponding to the homogeneous regime (large scale), and 0, corresponding to the extremely disordered fractal regime (small scale).

Finally, it is worth noting that the exponents of the three scaling laws in Eqs. (14), (16) and (17) are not independent. The relationship among them can be obtained by the integral definition of the crushing energy (Carpinteri et al., 2002), once Eqs. (14) and (17) are generalized to the whole softening regime, $\sigma \sim \sigma^* d^{-d_\sigma}$ and $w \sim \varepsilon^* d^{(1-d_\varepsilon)}$:

$$\mathcal{G}_C = \int_0^{w_c} \sigma \, dw \sim d^{1-d_\varepsilon-d_\sigma} \int_0^{\varepsilon^*_c} \sigma^* \, d\varepsilon^* = \mathcal{G}^*_C d^{1-d_\varepsilon-d_\sigma}. \tag{18}$$

Eq. (18) highlights the effect of the structural size on the crushing energy, as Eq. (16) does. Therefore, comparing Eqs. (16) and (18), the relation among the exponents reads:

$$d_\sigma + d_\varepsilon + d_\mathcal{G} = 1. \tag{19}$$

The fractal approach is now used to obtain a scale-independent fractal overlapping law from the experimental tests carried out by Carpinteri et al. (2011b) on rock specimens, whose stress–strain diagrams are shown in Fig. 9a. In the sequel, the size effects on the compressive strength are not considered, since this mechanical property presents a statistical dispersion, but not a clear size-effect. As a consequence, the exponent d_σ in Eq. (14) is taken equal to zero, and, therefore, Eq. (19) becomes:

$$d_\varepsilon + d_\mathcal{G} = 1. \tag{20}$$

In general, the value of the exponent $d_\mathcal{G}$ is given by the slope of the linear regression in the bi-logarithmic diagram representing the crushing energy – evaluated as the area beneath the stress vs. strain curves – as a function of the specimen size. Then, the value of the exponent d_ε is derived from Eq. (20). The normalized stress vs. fractal strain diagrams

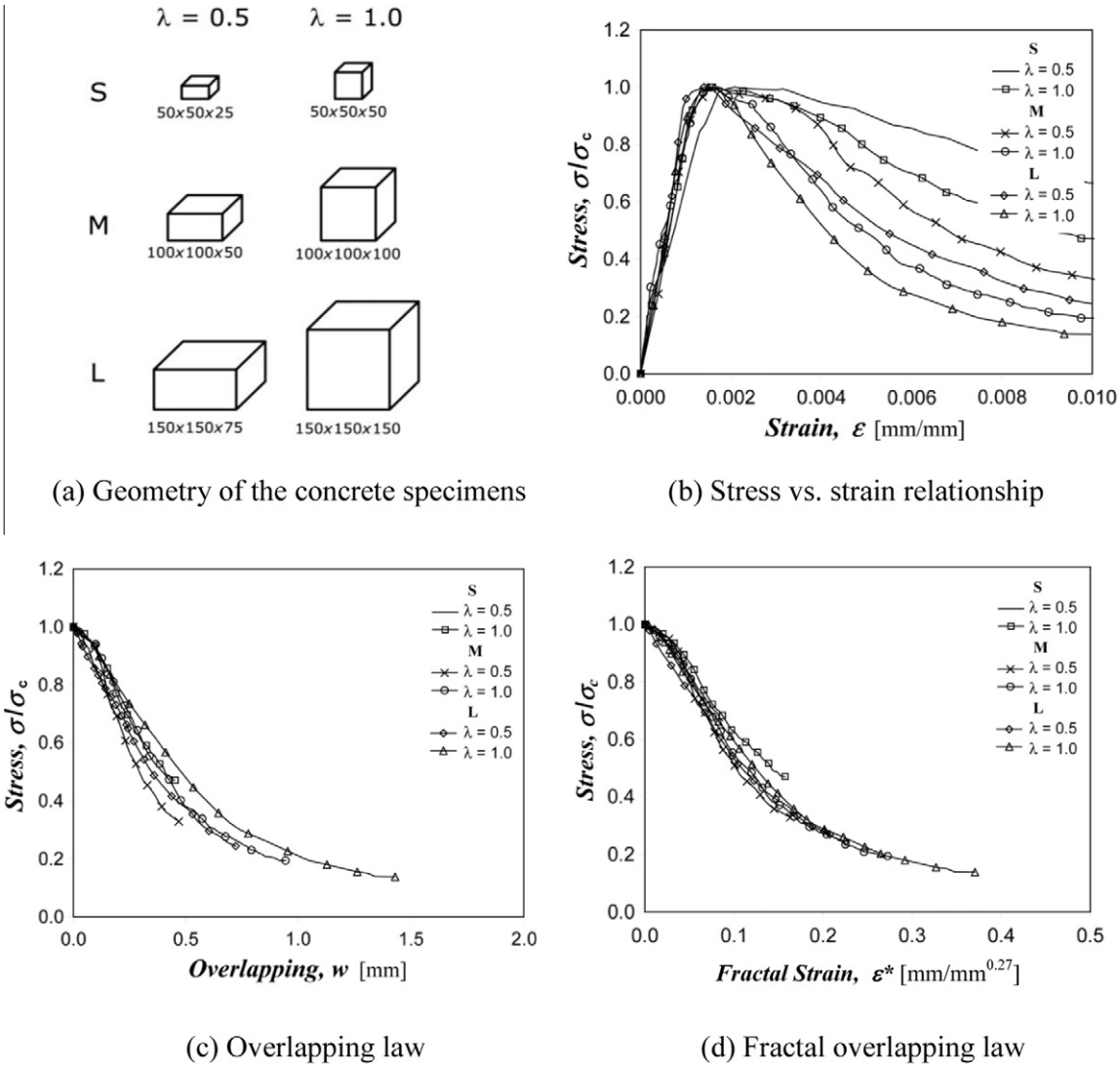

Fig. 11. Compression tests on concrete specimens by Ferrara and Gobbi (1995) (a); stress vs. strain diagrams (b); overlapping law diagrams (c) and fractal overlapping law diagrams (d).

obtained for the rock specimens herein considered are shown in Fig. 9c. As expected, a closer distribution of the different curves, with respect to the overlapping laws shown in Fig. 9b, is obtained, giving rise to the scale-independent (fractal) overlapping law. The values for the exponents $d_{\mathcal{G}}$ and d_{ε} that optimize the collapse of the curves are 0.30 and 0.70, respectively. Their physical meaning reveals that the energy dissipation takes place on a fractal domain of dimension 2.30 and the strain field presents a fractal pattern, the fractal strain, ε^*, assuming the anomalous dimension of $mm/mm^{0.30}$. Similar confirmations to the effectiveness of the fractal approach in determining scale-independent constitutive laws have been proposed for concrete specimens subjected to both tension (Carpinteri et al., 2002, 2006a) and compression (Carpinteri and Corrado, 2009). In the latter case, the stress–strain curves of the specimens with different size and slenderness tested by Ferrara and Gobbi (1995) have been analyzed (Fig. 11a and b). The obtained fractal overlapping law is characterized by a dimension of the fractal domain for the energy dissipation equal to 2.27, to which corresponds a fractal strain with physical dimension $L^{0.73}$ (see Fig. 11d). Such exponents are very similar to those obtained for the calcareous stone considered previously.

5. Applications of fractal damage models

Some applications of the AE fractal damage model, obtained on the basis of the energy density criterion of Eq. (5), are described in Carpinteri et al. (2007b) and Carpinteri and Lacidogna (2007). In these papers the fractal model is used for interpreting data obtained at the laboratory scale, and on full scale structures. In particular, the fractal exponent D, obtained from tests at the laboratory scale, is used

to predict a volume-effect on the maximum number of AE events corresponding to the achievement of a critical condition. The stability evaluation of real structures, is performed connecting the damage evolution, estimable by the dating and systematic survey, with the cumulative distribution of AE events in time. The extent of damage in structures mainly subject to dead loads, can be worked out from the AE data recorded on a reference specimen (subscript r) obtained from the structure and tested up to failure. Obviously, the fundamental assumption is that the damage level observed in the reference specimen is proportional to the level reached in the entire structure before monitoring is started. From Eq. (4) we get $N_{max} = N_{maxr}(V/V_r)^{D/3}$, from which we can obtain the critical number of AE counts, N_{max}, for the structure (Carpinteri et al., 2007b).

Moreover, the evolution of the damage fractal dimension D, assessed by means of the statistical interpretation of b-value variations (Eq. (7)), is fundamental for the prediction of a critical state achievement, also considering different loading conditions. From a practical point of view, this means that the damage condition of a real structure can be identified – without the need of laboratory sample tests – through the energy release domain obtained by means of AE monitoring and characterized by the b-value analysis. $D = 3.0$, which corresponds to the critical conditions $b = 1.5$, means that the energy release takes place through small defects homogeneously distributed throughout the volume, whereas $D = 2.0$, which corresponds to $b = 1.0$, means that energy release takes place on a fracture surface, identifying a situation of potential collapse (Carpinteri et al., 2008a, 2011b).

As regards the third proposed approach, the physical dimension of the damage pattern is one of the parameters necessary to define scale-invariant constitutive laws and true material properties. From a practical point of view, the scaling laws for the material parameters and their scale-invariant values can be obtained from experimental results on specimens having three different scales. Unfortunately, such constitutive laws are rather difficult to use in calculations due to the fact that non-integer dimensions are assumed for the mechanical parameters. This problem can be solved on the basis of a fractional calculus approach. Applications of such a method to continuum mechanics and fractal structures can be found in Mosolov (1994), Carpinteri and Mainardi (1997), Kolwankar (1998) and Carpinteri and Cornetti (2002). On the other hand, once the scale-invariant parameters and their scaling laws are known, the classical material parameters, namely energy density, ultimate strain and strength, can be determined as a function of the considered structural size. In this way, the properties obtained at the laboratory scale can be correctly extrapolated to the real structural scale.

6. Discussion and conclusions

In this paper, three different approaches have been proposed to evaluate the fractal dimension of the damage domain at the peak load and in the post-peak regime of disordered materials subjected to uniaxial compression. The first is an energy approach, since it permits to evaluate the damage domain fractality from the scaling of the energy release obtained from the cumulative number of AE events, N_{max}. From a practical point of view, it is obtained from the slope of the curve relating N_{max} to the specimen volume, in a bi-logarithmic diagram. The second method proposed is based on the b-value variation during the evolution of damage detected by AE. This variation is closely connected with the evolution of the damage domain fractality. According to experimental evidences on strain localization, in fact, the b-value decreases when the post-peak softening stage is approached, describing a localization of the energy release. Finally, a third method has been proposed, based on the renormalization group procedure applied to obtain scale-independent constitutive laws in compression. This result is achieved by assuming non-integer dimensions for the mechanical parameters, and therefore, for the domain of energy dissipation. Some applications of these fractal models to laboratory and full scale structures are also commented.

Moreover, in the case of the disordered materials analyzed in this paper, the three approaches have given very similar values for the D exponent, close to 2.30, without relevant differences between concrete and rocks. It is worth noting that such values have been obtained by analysing different parts of the load–displacement curve, i.e., the peak or the softening branch, depending on the different considered method. In this context, it has to be remarked that the energy approach is the only effective in the case of specimens exhibiting a very brittle behavior, characterized by a catastrophic collapse after the peak load and the lack of information about the softening branch of the load–displacement curve. The closeness of D to the value 2.0 confirms that also in heterogeneous materials the energy dissipation is a surface-dominated phenomenon, although only the fractal fracture energy can be assumed as a scale-independent parameter.

The non-perfect matching between the values obtained for the D exponent of a given material is due to the fact that different approaches can lead to underestimate or overestimate some measurements obtained during the tests. As a matter of fact, the damage fractal dimension D, calculated by Eq. (5), is obtained by a best-fitting of the N_{max} values arranged in bi-logarithmic scale for each specimen volume, whereas, the b-values, obtained by Eq. (7) are defined as the log-linear slope of the frequency-magnitude distribution of AE events. The two approaches, therefore, are completely different. Moreover, the b-value analysis takes into account not only the number of AE events, but also their amplitude. Damage, in fact, especially in the pre-peak branch of the load vs. time diagrams, advances with a considerable number of AE events having small amplitudes, that could result – if the statistics is limited to a single specimen – to an overestimation of the fractal domain D. This experimental evidence is also described in the fundamental paper by Lockner et al. (1991) in which it is observed that during triaxial compressive tests on granite and sandstone "the b-values for pre-nucleation events are indeed larger than for post-nucleation events, indicating a greater percentage of low amplitude events in the pre-nucleation phase".

Finally, the three proposed methods – energy density criterion, *b*-value analysis, and overlapping crack model – are defined as "indirect" because they permit to evaluate the damage domain fractal dimension on the basis of global parameters that can be easily detected during a standard compression test, such as, the stress–strain curve and the acoustic emission event number. On the contrary, the procedure of localization of the acoustic emission events, permits to identify the position within the specimen volume of the energy release sources, and, therefore, to directly assess the fractal dimension of the damage domain by means of the box counting method (Chelidze and Gueguen, 1990; Turcotte, 1997). Actually, the proposed empirical methods, even if indirect, should provide a *reasonable value* of the damage domain fractal dimension, although, from a practical point of view, the results are affected by the scatter in the experimental data.

Acknowledgements

The financial supports provided by the Ministry of University and Scientific Research (MIUR) to the project "Advanced applications of Fracture Mechanics for the study of integrity and durability of materials and structures", and by the Regione Piemonte to the RE-FRESCOS project: "Preservation, safeguard and valorisation of masonry decorations in the architectural historical heritage of Piedmont", are gratefully acknowledged.

References

Aki, A., 1981. A probabilistic synthesis of precursory phenomena. In: Simpson, D.W., Richards, P.G. (Eds.), Earthquake Prediction: An International Review, M. Ewing Series, vol. 4, pp. 566–574.

Carpinteri, A., 1986. Mechanical Damage and Crack Growth in Concrete: Plastic Collapse to Brittle Fracture. Martinus Nijhoff Publishers, Dordrecht.

Carpinteri, A., 1994a. Scaling laws and renormalization groups for strength and toughness of disordered materials. Int. J. Solids Struct. 31, 291–302.

Carpinteri, A., 1994b. Fractal nature of material microstructure and size effects on apparent mechanical properties. Mech. Mater. 18, 89–101.

Carpinteri, A., Cornetti, P., 2002. A fractional calculus approach to the description of stress and strain localization in fractal media. Chaos Soliton Fract. 13, 85–94.

Carpinteri, A., Corrado, M., 2009. An extended (fractal) Overlapping Crack Model to describe crushing size-scale effects in compression. Eng. Fail. Anal. 16, 2530–2540.

Carpinteri, A., Lacidogna, G., 2007. Damage evaluation of three masonry towers by acoustic emission. Eng. Struct. 29, 1569–1579.

Carpinteri, A., Mainardi, F., 1997. Fractals and fFractional Calculus in Continuum Mechanics. Springer, Wien.

Carpinteri, A., Pugno, N., 2002a. Fractal fragmentation theory for shape effects of quasi-brittle materials in compression. Mag. Concr. Res. 54, 473–480.

Carpinteri, A., Pugno, N., 2002b. A fractal comminution approach to evaluate the drilling energy dissipation. Int. J. Numer. Anal. Methods Geomech. 26, 499–513.

Carpinteri, A., Chiaia, B., Invernizzi, S., 1999. Three-dimensional fractal analysis of concrete fracture at the meso-level. Theor. Appl. Fract. Mech. 31, 163–172.

Carpinteri, A., Chiaia, B., Cornetti, P., 2002. A scale-invariant cohesive crack model for quasi-brittle materials. Eng. Fract. Mech. 69, 207–217.

Carpinteri, A., Cornetti, P., Puzzi, S., 2006a. Scaling laws and multiscale approach in the mechanics of heterogeneous and disordered materials. Appl. Mech. Rev. (ASME) 59, 283–305.

Carpinteri, A., Lacidogna, G., Niccolini, G., 2006b. Critical behaviour in concrete structures and damage localization by acoustic emission. Key Eng. Mater. 312, 305–310.

Carpinteri, A., Corrado, M., Paggi, M., Mancini, G., 2007a. Cohesive versus overlapping crack model for a size effect analysis of RC elements in bending. In: Carpinteri, A., Gambarova, P., Ferro, G., Plizzari, G. (Eds.), Fracture Mechanics of Concrete Structures (Proceedings FraMCoS-6), vol. 2. Taylor & Francis, London, pp. 655–663.

Carpinteri, A., Lacidogna, G., Pugno, N., 2007b. Structural damage diagnosis and life-time assessment by acoustic emission monitoring. Eng. Fract. Mech. 74, 273–289.

Carpinteri, A., Lacidogna, G., Niccolini, G., Puzzi, S., 2008a. Critical defect size distributions in concrete structures detected by the acoustic emission technique. Meccanica 43, 349–363.

Carpinteri, A., Lacidogna, G., Puzzi, S., 2008b. Prediction of cracking evolution in full scale structures by the *b*-value analysis and Yule statistics. Phys. Mesomech. 11, 260–271.

Carpinteri, A., Corrado, M., Mancini, G., Paggi, M., 2009a. The overlapping crack model for uniaxial and eccentric concrete compression tests. Mag. Concr. Res. 61, 745–757.

Carpinteri, A., Lacidogna, G., Niccolini, G., 2009b. Fractal analysis of damage detected in concrete structural elements under loading. Chaos Soliton Fract. 42, 2047–2056.

Carpinteri, A., Lacidogna, G., Puzzi, S., 2009c. From criticality to final collapse: evolution of the *b*-value from 1.5 to 1.0. Chaos Soliton Fract. 41, 843–853.

Carpinteri, A., Cardone, F., Lacidogna, G., 2010. Energy emissions from failure phenomena: mechanical, eletromagnetic, nuclear. Exp. Mech. 50, 1235–1243.

Carpinteri, A., Corrado, M., Paggi, M., 2011a. An analytical model based on strain localization for the study of size-scale and slenderness effects in uniaxial compression tests. Strain 47, 351–362.

Carpinteri, A., Lacidogna, G., Manuello, A., 2011b. The *b*-value analysis for the stability investigation of the ancient Athena temple in Syracuse. Strain 47, e243–e253.

Chelidze, T., Gueguen, Y., 1990. Evidence of fractal fracture. Int. J. Rock Mech. Min. Sci. Geomech. Abstr. 27, 223–225.

Colombo, S., Main, I.G., Forde, M.C., 2003. Assessing damage of reinforced concrete beam using "*b*-value" analysis of acoustic emission signals. J. Mater. Civil Eng. ASCE 15, 280–286.

Ferrara, G., Gobbi, M.E., 1995. Strain softening of concrete under compression. Report to RILEM Committee 148 SCC, ENEL-CRIS Laboratory, Milano, Italy.

Garcimartin, A., Guarino, A., Bellon, L., Ciliberto, S., 1997. Statistical properties of fracture precursors. Phys. Rev. Lett. 79, 3202.

Hirata, T., 1989. A correlation between *b*-value and the fractal dimension of earthquakes. J. Geophys. Res. 94, 7507–7514.

Hudson, J.A., Brown, E.T., Fairhurst, C., 1972. Shape of the complete stress–strain curve for rock. In: Cording, E.J. (Ed.), Stability of Rock Slopes (Proceedings of the 13th Symposium on Rock Mechanics). American Society of Civil Engineers, New York, pp. 773–795.

Jansen, D.C., Shah, S.P., 1997. Effect of length on compressive strain softening of concrete. J. Eng. Mech. 123, 25–35.

King, G.C.P., 1983. The accommodation of large strains in the upper lithosphere of the earth and other solids by self-similar fault systems: the geometrical origin of *b*-value. Earth Pure Apply Geophys. 121, 761–815.

Kleiser, T., Bocek, M., 1986. The fractal nature of slip in crystals. Z. Metallkd. 77, 582–587.

Kolwankar, K.M., 1998. Studies of Fractal Structures and Processes using Methods of Fractional Calculus. Ph.D. Thesis. University of Pune, India.

Kotsovos, M.D., 1983. Effect of testing technique on the post-ultimate behaviour of concrete in compression. Mater. Struct. 16, 3–12.

Krajcinovic, D., Rinaldi, A., 2005. Statistical damage mechanics – 1. Theor. J. Appl. Mech. 72, 76–85.

Lockner, D.A., Byerlee, J.D., Kuksenko, V., Ponomarev, A., Sidorin, A., 1991. Quasi static fault growth and shear fracture energy in granite. Nature 350, 39–42.

Lu, C., Mai, Y-W., Shen, Y-G., 2005. Optimum information in crackling noise. Phys. Rev. E 72, 027101-1.

Main, I.G., 1991. A modified Griffith criterion for the evolution of damage with a fractal distribution of crack lengths: Application to seismic event rates and b-values. Geophys. J. Int. 107, 353–362.

Main, I.G., 1992. Damage mechanics with long-range interactions: correlation between the seismic *b*-value and the two point correlation dimension. Geophys. J. Int. 111, 531–541.

Main, I.G., 2000. A damage mechanics model for power-law creep and earthquake aftershock and foreshock sequences. Geophys. J. Int. 142, 151–161.

Mandelbrot, B.B., 1982. The fractal geometry of nature. Freemann and Company, New York.

Mandelbrot, B.B., Passoja, D.E., Paullay, A.J., 1984. Fractal character of fracture surfaces of metals. Nature 308, 721–722.

Mosolov, A., 1994. Singular fractal functions and mesoscopic effects in mechanics. Chaos Soliton Fract. 4, 2093–2102.
Ohtsu, M., 1996. The history and development of acoustic emission in concrete engineering. Mag. Concr. Res. 48, 321–330.
Panin, V.E., Elsukova, T., Angelova, G., Kuznetsov, P., 2002. Mechanism of formation of fractal mesostructure at the surface of polycrystals upon cyclic loading. Phys. Metals Metallogr. 94, 402–412.
Poliakov, A.N.B., Hermann, H.J., Podladchikov, Y.Y., Roux, S., 1995. Fractal plastic shear bands. Fractals 2, 567–581.
Rao, M.V.M.S., Prasanna Lakshmi, K.J., 2005. Analysis of *b*-value and improved *b*-value of acoustic emissions accompanying rock fracture. Curr. Sci. 89, 1577–1582.
Richter, C.F., 1958. Elementary Seismology. W.H. Freeman, San Francisco, London.
Rinaldi, A., Mastilovic, S., Krajcinovic, D., 2006. Statistical damage mechanics – 2. Constitutive relations. J. Theor. Appl. Mech. 44, 585–602.
Rundle, J.B., Turcotte, D.L., Shcherbakov, R., Klein, W., Sammis, C., 2003. Statistical physics approach to understanding the multiscale dynamics of earthquake fault systems. Reviews of Geophysics 41, 1–30.
Sammonds, P.R., Meredith, P.G., Murrel, S.A.F., Main, I.G., 1994. Modelling the damage evolution in rock containing porefluid by acoustic emission, in: Proceedings of the Eurock'94, Balkema, Rotterdam, The Netherlands.
Scholz, C.H., 1968. The frequency–magnitude relation of microfracturing in rock and its relation to earthquakes. Bull. Seismol. Soc. Am. 58, 399–415.
Sethna, J.P., Dahmen, K.A., Myers, C.R., 2001. Crackling noise. Nature 410, 242.
Turcotte, D.L., 1997. Fractals and Chaos in Geology and Geophysics. Cambridge University Press, New York.
van Mier, J.G.M., 1984. Strain softening of concrete under multiaxial compression. PhD Thesis. Eindhoven University of Technology, The Netherlands.
Weiss, J., Marsan, D., 2003. Three-dimensional mapping of dislocation avalanches: clustering and space/time coupling. Science 299, 89–92.